Mon. Not. R. Astron. Soc. **367,** 599–610 (2006) doi:10.1111/j.1365-2966.2005.09930.x

First estimates of the fundamental parameters of the relatively bright Galactic open cluster NGC 5288

Andrés E. Piatti,[1⋆] Juan J. Clariá[2⋆] and Andrea V. Ahumada[2⋆]
[1]*Instituto de Astronomía y Física del Espacio, CC 67, Suc. 28, 1428 Ciudad de Buenos Aires, Argentina*
[2]*Observatorio Astronómico, Universidad Nacional de Córdoba, Laprida 854, 5000 Córdoba, Argentina*

Accepted 2005 November 28. Received 2005 November 15; in original form 2005 October 31

ABSTRACT

In this paper we present charge-coupled device (CCD) images in the Johnson B and V and Kron–Cousins I passbands for the previously unstudied open cluster NGC 5288. The sample consists of 15 688 stars reaching down to $V \sim 20.5$. The cluster appears to have a relatively small but conspicuous nucleus and a low-density extended coronal region. Star counts carried out in 25×25 pixel^2 boxes distributed throughout the whole observed field allowed us to estimate the angular core and corona radii as ∼1.3 and 6.3 arcmin, respectively. Our analysis suggests that NGC 5288 is moderately young and probably more metal-rich than the Sun. Adopting the theoretical metal content $Z = 0.040$, which provides the best global fit, we derive an age of 130^{+40}_{-30} Myr. Simultaneously, we have obtained colour excesses $E(B-V) = 0.75$ and $E(V-I) = 0.95$ and an apparent distance modulus $V - M_V = 14.00$. The law of interstellar extinction in the cluster direction is found to be normal. NGC 5288 is located at 2.1 ± 0.3 kpc from the Sun beyond the Carina spiral feature and ∼7.4 kpc from the Galactic Centre. The cluster metallicity seems to be compatible with the cluster position in the Galaxy, given the recognized radial abundance gradient in the disc. For the first time, in this paper we determine the basic parameters for the open cluster NGC 5381, situated in the same direction as NGC 5288. This determination was reached by using CCD VI data published almost a decade ago by Pietrzyński et al. (1997) for NGC 5381. The properties of some open clusters aligned along the line of sight of NGC 5288 are examined. The properties of clusters of similar ages to NGC 5288 are also looked into. Evidence is presented that these did not form mainly along the spiral arms but rather in the thin Galactic disc ($Z \sim \pm 100$ pc).

Key words: techniques: photometric – open clusters and associations: general – open clusters and associations: individual: NGC 5288.

1 INTRODUCTION

It is generally accepted (see e.g. Friel 1995) that open clusters are fundamental landmarks to probe Galaxy properties. They are among the very few Galactic objects for which meaningful distances can be derived over a large range, which makes them an essential tool to constrain Galactic evolution theories. They also provide more accurate ages than do other disc objects. Therefore, the study of the Galactic open cluster system proves very useful to clarify the many queries concerning our Galaxy's structure (Janes & Adler 1982; Friel 1995) and evolution (Friel & Janes 1993; Chen, Hou & Wang 2003).

The present paper is one of a series devoted to some unstudied or poorly studied open clusters located in different regions of the Milky Way. Our goal is to obtain good-quality charge-coupled device (CCD) photometric data, not only to produce a larger sample of studied open clusters, but also to determine their fundamental parameters accurately, using the most recent family of theoretical isochrones. We have already reported results on the relatively young clusters NGC 2194, 2324 and 6318 (Piatti, Clariá & Ahumada 2003a, 2004a, 2005a), on the Hyades-like cluster Lyngå 11 (Piatti, Clariá & Ahumada 2006), on the intermediate-age clusters NGC 2627 and Tombaugh 1 (Piatti, Clariá & Ahumada 2003b, 2004b), and on the old, metal-poor anticentre cluster Trumpler 5 (Piatti, Clariá & Ahumada 2004c).

The cluster of our current interest is NGC 5288, also designated as C1345−644, Cr 278 (Collinder 1931) or BH 153 (van den Bergh & Hagen 1975). It is number 910 in the catalogue of Alter, Ruprecht & Vanisek (1970) and is included in Hogg's (1965) Atlas of Southern Open Clusters, wherein it appears rather faint for its angular diameter. NGC 5288 is located in Circinus at $\alpha_{2000} = 13^{\rm h}48^{\rm m}46^{\rm s}$, $\delta_{2000} = -64^\circ 41' 11''$, with Galactic coordinates $l = 309\overset{\circ}{.}01$ and $b = -2\overset{\circ}{.}49$.

⋆E-mail: andres@iafe.uba.ar (AEP); claria@mail.oac.uncor.edu (JJC); andrea@mail.oac.uncor.edu (AVA)

Table 1. Sample CCD *BVI* data of stars in the field of NGC 5288.[a] (This table is available for download in its entirety as part of the full-text version of the article from http://www.blackwell-synergy.com.)

Star	X (pixel)	Y (pixel)	V (mag)	$\sigma(V)$ (mag)	n_V	$B-V$ (mag)	$\sigma(B-V)$ (mag)	n_{B-V}	$V-I$ (mag)	$\sigma(V-I)$ (mag)	n_{V-I}
574	1427.942	57.662	16.160	0.018	3	0.892	0.037	3	1.153	0.045	3
575	355.763	57.669	17.681	0.078	3	1.299	0.039	3	1.780	0.036	3
576	2005.710	57.696	17.466	0.015	3	1.451	0.044	3	1.920	0.072	3
...	...	...	...	...	...	...	...	...	...	...	...
...	...	...	...	...	...	...	...	...	...	...	...

[a]The (X, Y) coordinates correspond to the reference system of Fig. 1. Magnitude and colour errors are the standard deviations of the mean, or the observed photometric errors for stars with only one measurement.

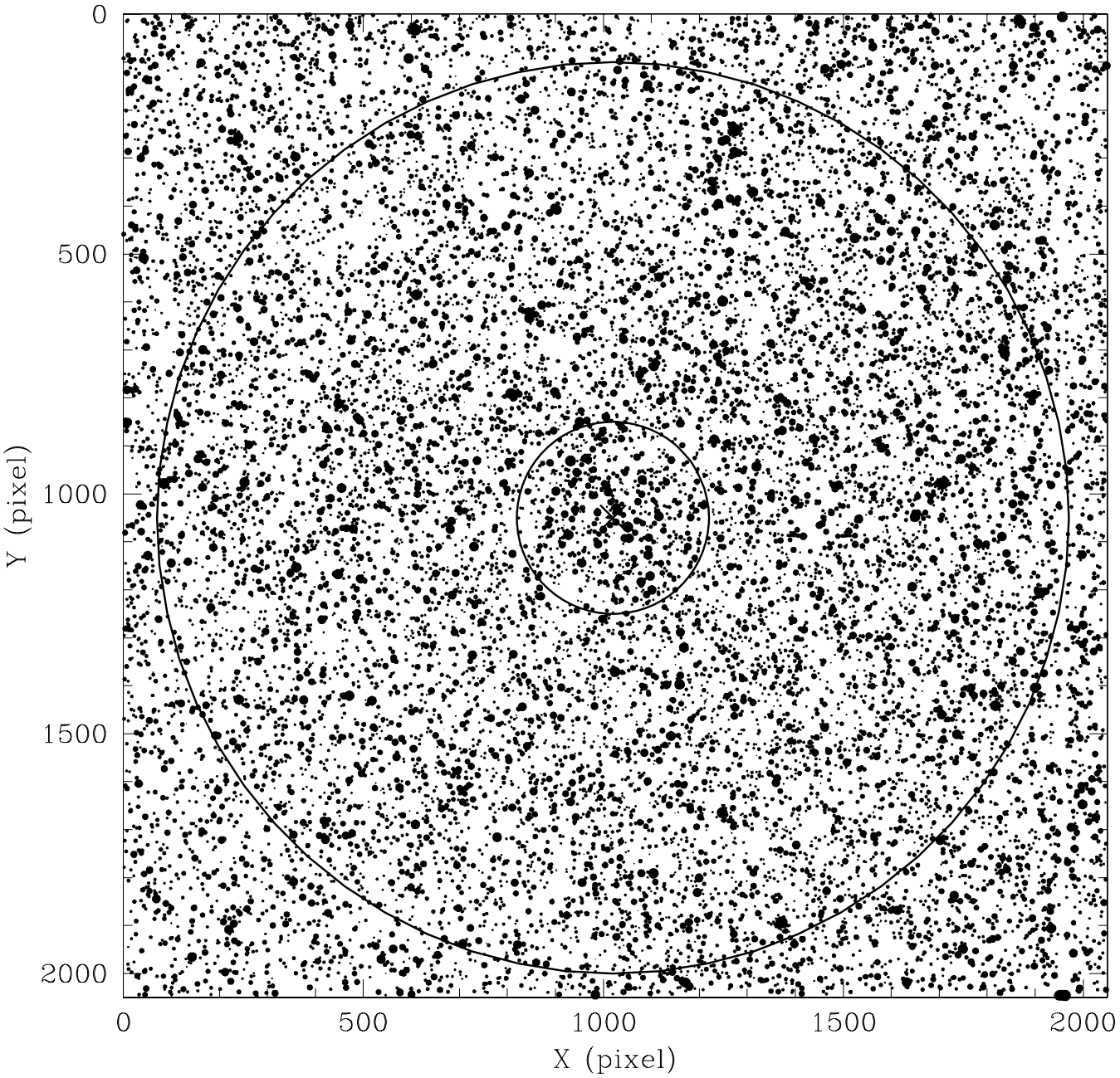

Figure 1. Schematic finding chart of the stars observed in the field of NGC 5288. North is up and east is to the left. The sizes of the plotting symbols are proportional to the V brightness of the stars. Two concentric circles 200 and 950 pixels wide around the cluster centre (cross) are shown.

The Lund Catalogue of Open Cluster Data (Lyngå 1987) describes it as a slightly concentrated cluster with 25 members and an angular diameter of 3 arcmin as measured from the POSS charts. Ruprecht (1966) refers to this small-sized open cluster as belonging to Trumpler class II-2p (Trumpler 1930), i.e. a poor, detached cluster with little central concentration and medium-range bright stars. However, Archinal & Hynes (2003) recently classified it as a II-1p system. Old distance determinations by Trumpler (1930), Collinder (1931) and Barkhatova (1950) place the cluster as lying between 2.0 and 7.2 kpc from the Sun.

No parameters are currently available for this cluster according to the WEBDA Open Cluster Database (Mermilliod 2005). Therefore, the present work attempts to shed light on the nature of this object by means of CCD photometry, by determining for the first time its size, reddening, distance, age and metallicity.

Section 2 briefly describes the observations and data reduction. The data quality as well as some structural cluster features such as the extension of the core radius and the cluster corona are discussed in Section 3. In Section 4 we present a description and analysis of the main features appearing in the colour–magnitude diagrams (CMDs). In Section 5 we determine the fundamental cluster parameters through the fitting of theoretical isochrones. In Section 6 we examine the properties of a sample of open clusters located towards the direction of NGC 5288, using the WEBDA Open Cluster Database (Mermilliod 2005). The final section provides our conclusions and a brief summary of the results.

2 DATA ACQUISITION AND REDUCTION PROCEDURES

The NGC 5288 field was observed on 1998 June 19–20 with the Cerro Tololo Inter-American Observatory (CTIO) 0.9-m telescope and with the Tektronix 2K #3 CCD, using quad-amp readout. Given that the cluster was observed during the same run as NGC 6318, an open cluster whose analysis was published by Piatti et al. (2005a), we refer the reader to that paper for a detailed description of the data acquisition and reduction procedure. A master table was produced containing the average values of V, $B-V$ and $V-I$ with their errors $\sigma(V)$, $\sigma(B-V)$ and $\sigma(V-I)$ and the independent number of observations $n_{\rm V}$, $n_{\rm B-V}$ and $n_{\rm V-I}$ for each star, respectively. We derived magnitudes and colours for a total of 15 688 stars in the field of NGC 5288. Table 1 presents this information. Only a fragment of this table is shown here in the printed version for guidance regarding its form and content; it is available in its entirety in the online version of the journal on *Synergy*.

3 DATA HANDLING

3.1 Data quality and scopes

A simple inspection of Table 1 shows that 47 and 54 per cent, respectively, of the total number of stars with $B-V$ and $V-I$ colours have three measures, and expand from the brightest limit down to

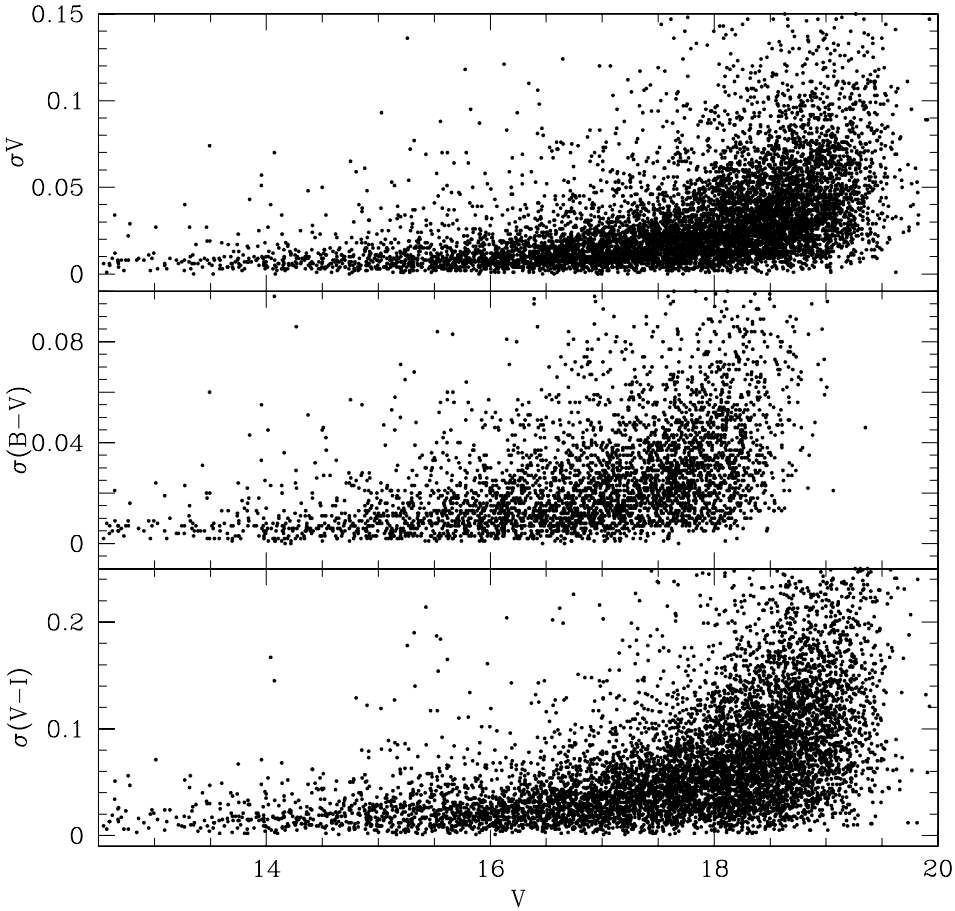

Figure 2. Magnitude and colour photometric errors as a function of V.

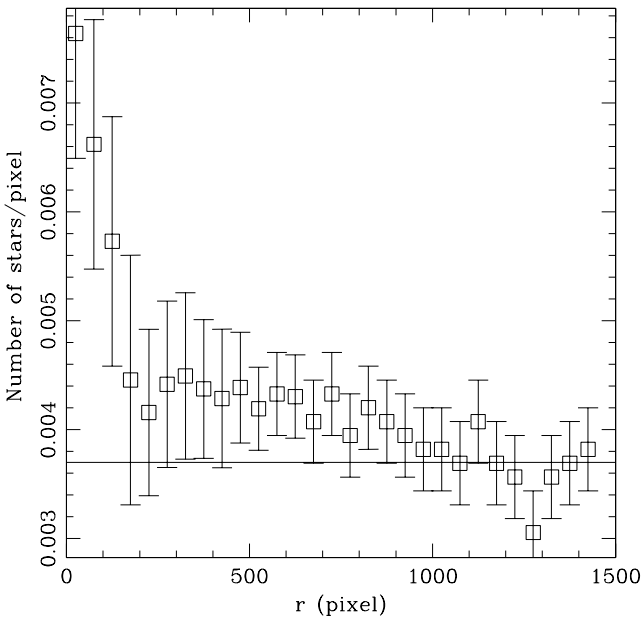

Figure 3. Stellar density profile centred at $(X_C, Y_C) = (1020, 1050)$ pixel for stars observed in the field of NGC 5288. The horizontal line represents the background level measured for $r > 1000$ pixels.

$V = 18.5$ mag $(B - V)$ and 19.5 mag $(V - I)$. We have found no clear signs of variability among these stars. Two measures of $B - V$ and $V - I$ colours occur for 22 and 20 per cent of the stars and cover V ranges from 18 to 19.5 mag and from 18.5 to 20 mag, respectively. One measure in $B - V$ and $V - I$ applies to 31 and 26 per cent; all these stars being fainter than 18.5 mag $(B - V)$ and 19.5 mag $(V - I)$ up to the photometric magnitude limits, which are placed one magnitude below. According to these crude statistics, most of the ∼8 mag along which our photometry extends is covered by stars measured three times. This way of handling the photometric data supports the reliability of the subsequent photometric analysis. At the same time, we have approximately half of the measured stars (with one and two measures) distributed within the two faintest magnitudes reached. Such a result reveals that the field of NGC 5288 (Fig. 1) contains plenty of relatively faint stars, which probably constitute the background of the cluster.

The photometric errors provided by the standard deviation of the mean for the V magnitude and $B - V$ and $V - I$ colours have been plotted against their corresponding V magnitudes in Fig. 2. We use stars that exhibit three measures, since they more clearly show how tightly the standard photometric system is reproduced. By using photometric errors provided by DAOPHOT (only one measure per star), we obtain similar diagrams with a reasonably small intrinsic scatter. On the other hand, since the stars with three measures cover most of the dynamic magnitude range, they are the most

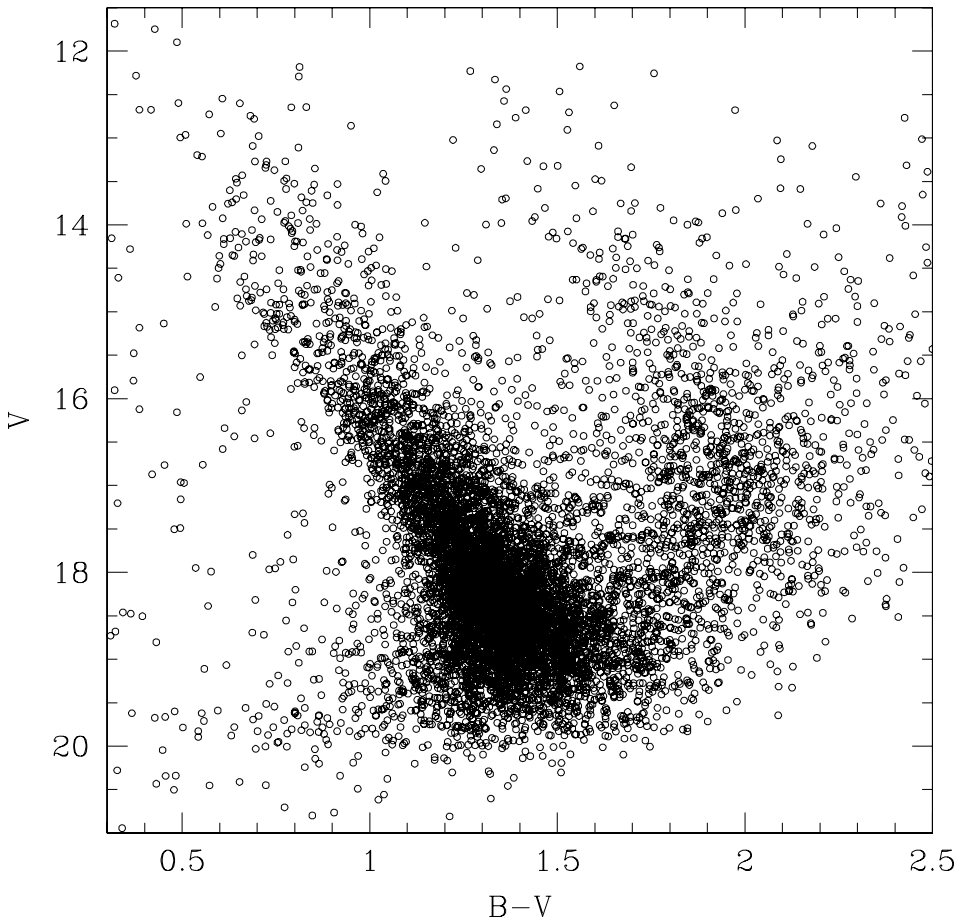

Figure 4. The $(V, B - V)$ colour–magnitude diagram for stars observed in the field of NGC 5288.

appropriate ones from which to derive astrophysical information. In addition, knowledge of the behaviour of the photometric errors with the magnitude for these stars allows us to rely on the accuracy of the morphology and position of the main cluster features in the CMDs.

3.2 Structural cluster features

NGC 5288 should be easily identifiable within the crowded star field. However, since distinct small groups of stars can be mistaken for the cluster centre (see Fig. 1), we decided to determine the cluster central position statistically. The strategy to determine the cluster centre consisted in tracing the stellar density profiles projected on to the directions of the X- and Y-axes, and in obtaining the coordinates associated to the peak of the stellar density distribution by fitting those profiles. In order to build the X projected density profile, we counted the number of stars distributed along fringes of a fixed width and oriented along the Y-axis. Similarly, the Y projected density profile was constructed using fringes placed along the X-axis. The width of the fringes was fixed at 25 pixels for both axes. This value results in a compromise between minimizing spurious effects, mainly caused by the presence of localized groups, rows or columns of stars, and maximizing the spatial resolution. The range of useful bin sizes is also constrained by the mean field stellar density, which translates into a lower limit for the mean free path between two stars. We chose a relatively small interval because the field is too crowded.

The projected stellar density profiles were fitted using the NGAUSSFIT routine of the STSDAS IRAF package. We adopted the multiple Gaussian fitting option, fixed the constant and linear terms to the corresponding background level and to zero, respectively, and set the number of matching Gaussians to one. The centre of the Gaussian, its amplitude and its full width at half-maximum (FWHM) acted as variables. We iterated the fitting procedure once on average, after eliminating a couple of dispersed points. We compared the resulting values with the cluster centre, estimated by eye looking at the cluster finding chart. The final coordinates for the cluster centre, marked by a cross in Fig. 1, turned out to be $(X_C, Y_C) = (1020 \pm 50, 1050 \pm 50)$ pixel, which were adopted in the following analysis.

We built the cluster radial profile with the multiple aims of: (i) estimating the cluster radius, generally used as an indicator of the cluster dimension; (ii) examining the extension of the cluster core and corona; and (iii) establishing the area out of which field stars practically prevail. The availability of a field area is highly valued, mainly because it helps to disentangle fiducial cluster and field features in the observed CMD. The most common way of building the cluster stellar density radial profile consists in counting the number of stars distributed in concentric rings around the cluster centre and normalizing the sum of stars in each ring to unit area. This procedure allows the observer to stretch easily the radial profile as much as possible until complete circles can be traced in the observed field. However, and in order to move even further away from the cluster centre, we decided to follow another method based on counts of stars located in boxes of 25 pixels a side, which are spread throughout

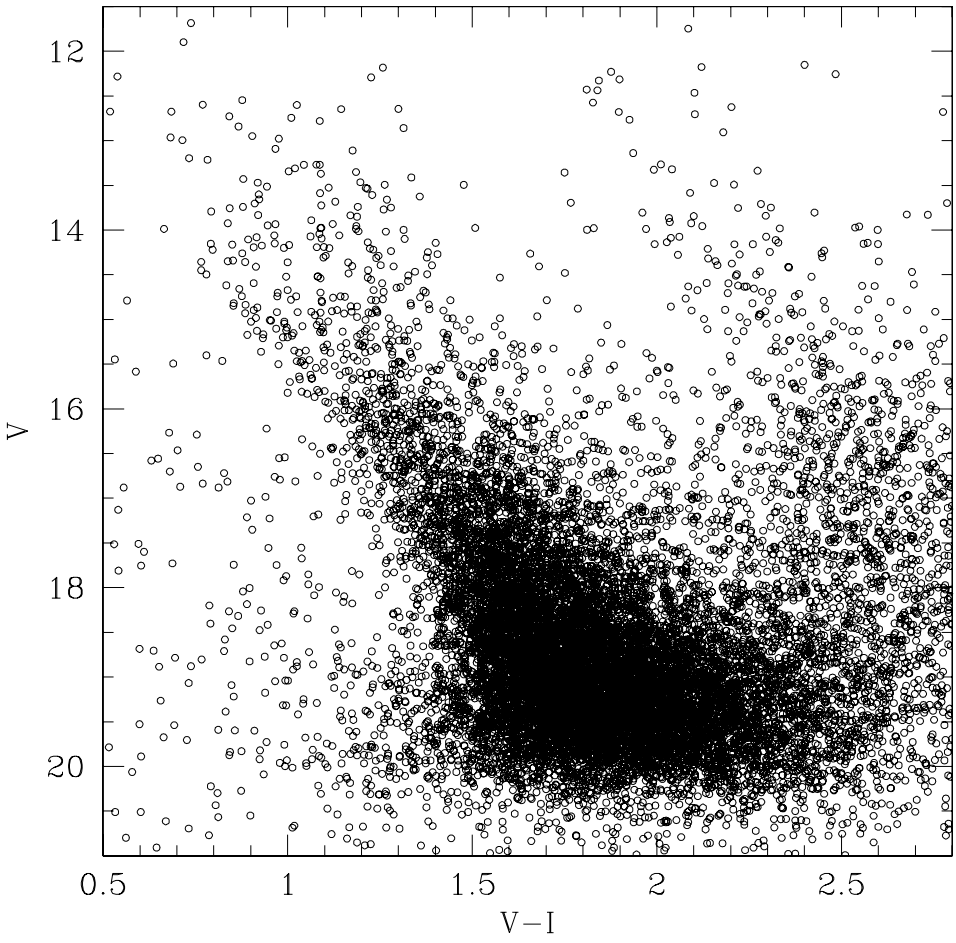

Figure 5. The $(V, V - I)$ colour–magnitude diagram for stars observed in the field of NGC 5288.

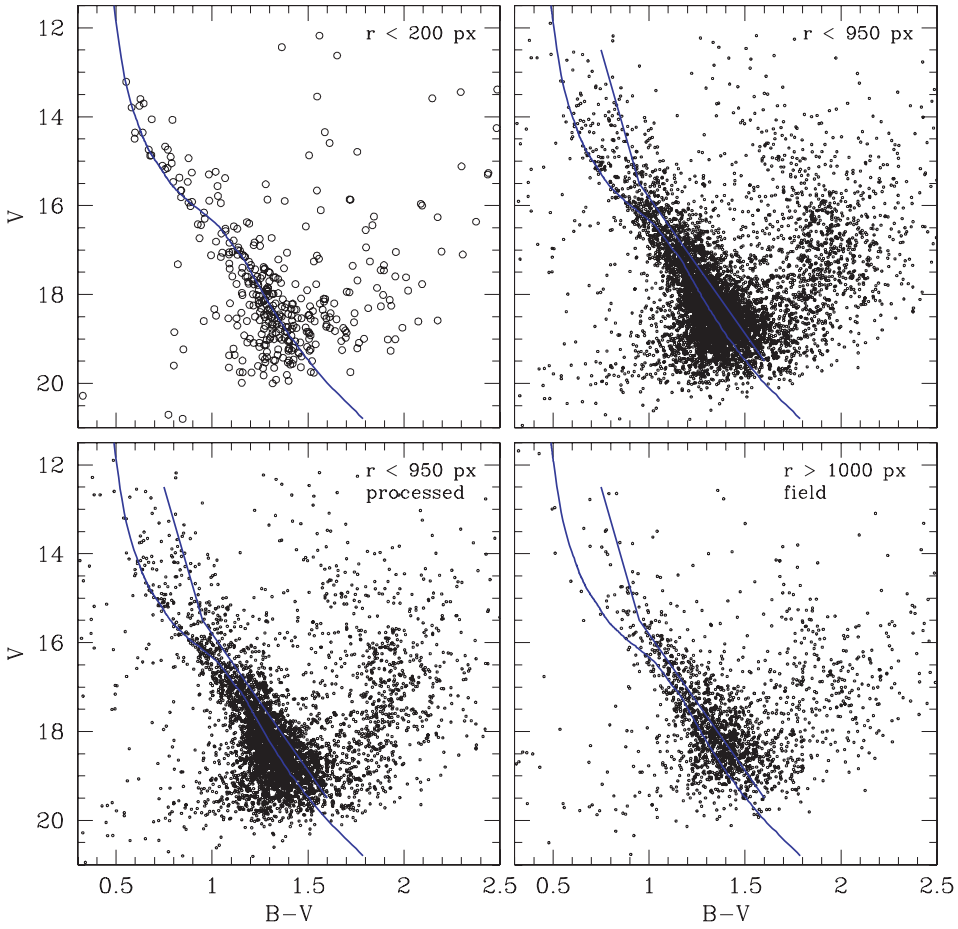

Figure 6. The $(V, B-V)$ colour–magnitude diagrams for stars observed in different extracted regions as indicated in each panel. The zero-age main sequence ($Z = 0.04$) from Lejeune & Schaerer (2001) and the fiducial main sequence of the cluster surrounding field are also shown. See Section 3.3 for details.

the whole field. Thus, the number of stars per unit area at a given radius r can be directly calculated through the expression

$$(n_{r+25} - n_{r-25})/\left[(m_{r+25} - m_{r-25}) \times 50^2\right],$$

where n_j and m_j, respectively, represent the number of counted stars and centres of boxes of 50 pixels a side included in a circle of radius j. The resulting stellar density profile is shown in Fig. 3. Note that in order to estimate the mean stellar density at that distance, this method does not necessarily require a complete circle of radius r within the observed field. Furthermore, instead of tracing the radial profile of NGC 5288 out to ∼1000 pixels (the radius of the largest complete circle that can be traced in the observed field), we obtained a cluster stellar density profile that extends up to 1500 pixels from its centre, as shown in Fig. 3.

With the aim of estimating the uncertainties in the derived stellar density profile, we proceeded as follows: First, we divided the observed field into angular sections 20 degrees wide, with the apex in the cluster centre. Then, we counted the number of stars lying in each angular section by using the method to obtain the cluster radial density profile described above. Next, we averaged the resulting stellar density profiles for all the angular sections – each angular section points to a different direction from the cluster centre – and finally we computed the standard deviation of the mean. We used the resulting standard errors to draw the error bars in Fig. 3. As can be seen, the more inwards a radius, the larger the error bars. This is due to the non-uniform distribution of cluster stars.

We used the error bars as a secondary reference to fit the background level at 0.0037 pixel^{-1}, and to adopt for the subsequent analysis the area for $r > 1000$ pixels as the 'star field area'. The mean stellar density in the field area proves to be slightly lower than half of the central cluster density. The horizontal line in Fig. 3 represents the derived background level. From this figure, we also estimated a cluster radius of 950 ± 50 pixels, equivalent to 6.3 ± 0.3 arcmin. NGC 5288 appears to have a relatively small but conspicuous nucleus of ∼200 pixels (∼1.3 arcmin) and a low-density extended corona (see also Fig. 1). Within the corona, it seems that there exist clumps of stars, as also is the case in the open cluster M67 (Chupina & Vereshchagin 1998). van den Bergh & Hagen (1975) derived a cluster radius of 3 arcmin from their survey of clusters in the southern Milky Way. Although they confirmed the reality of the cluster, they also mentioned that the cluster is questionably visible in the B and R plates. We think that the combination of a relatively crowded field and the extended low-density corona may account for the underestimation of the cluster dimension, on the part of the authors.

The existence of coronae in open clusters is well documented. Nilakshi Sagar et al. (2002) studied the relation between the core and the corona in Galactic star clusters, considering the density profiles of 38 rich open star clusters built using the Digital Sky Survey. Their study shows that the corona, most probably, is the outer region around the clusters. It also shows that the corona can exist from the very beginning of cluster formation and that dynamic

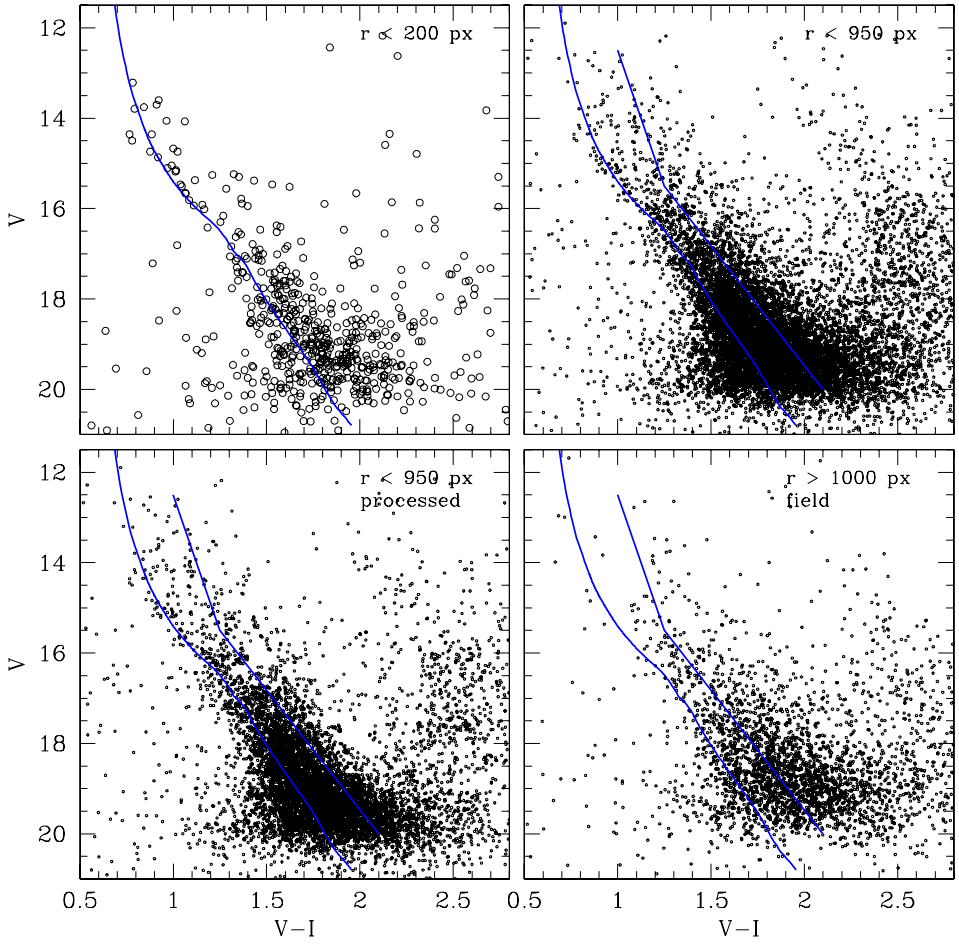

Figure 7. The $(V, V-I)$ colour–magnitude diagrams for stars observed in different extracted regions as indicated in each panel. The zero-age main sequence ($Z = 0.04$) from Lejeune & Schaerer (2001) and the fiducial main sequence of the cluster surrounding field are also shown. See Section 3.3 for details.

evolution is not the reason for its occurrence. Nilakshi Sagar et al. (2002) also found that the average value of the ratio between the core radius and the annular width of the corona is 4.3 ± 1.9. For NGC 5288, we derived a ratio of 3.6, which is in good agreement with the mean value derived by Nilakshi Sagar et al.

4 COLOUR–MAGNITUDE DIAGRAM FEATURES

Figs 4 and 5 show the resulting $(V, B-V)$ and $(V, V-I)$ CMDs, respectively, obtained using all the measured stars. A first glance at the figures reveals a crowded broad sequence of stars that traces the cluster main sequence (MS) along ∼6 mag and with clear evidence of some evolution. This fact suggests that the age of the cluster is some hundred million years. No clump of red stars is visible. According to Fig. 2, $\sigma_V \leqslant 0.05$ mag for $V = 19$ and ≈0.01 mag for $V < 17$; $\sigma_{B-V} \leqslant 0.05$ mag for $V = 18$ and 0.01 mag for $V < 16$; and $\sigma_{V-I} \leqslant 0.05$ mag for $V = 18.5$ and 0.01 mag for $V < 16.5$. Thus, the scatter produced by photometric errors is negligible in comparison with the colour width of the MS.

The blurred appearance of the cluster MS is mainly due to a remarkable contamination of inner Galactic disc stars, particularly the upper envelope of the MS. Most of those field stars are grouped in a redder sequence roughly shifted from the cluster MS that extends fairly parallel to it. Although this sequence appears to overlap the cluster MS, the position and shape of the latter are still distinguishable. If we continue upwards in magnitude from the field star sequence, younger field MS stars are also visible along a barely tilted sequence with some colour dispersion.

Field star contamination in the core and corona of an open cluster is on average ∼35 per cent and 80 per cent, respectively (Nilakshi Sagar et al. 2002). On the other hand, in spite of the relatively low densities in the cluster coronal region, it contains ∼75 per cent of the cluster members since its area is larger if compared to the core region. This clearly demonstrates the importance of the coronal region in studies dealing with the entire stellar contents of open star clusters as well as their dynamic evolution. For the above reasons, attempts at cleaning the cluster CMD from field stars are considered important.

With that aim in mind, we built CMDs from different circular extractions centred on the cluster. The radii of the circular extractions were chosen to obtain the best representation of the surrounding field stars, core and corona. Figs 6 and 7 show the extracted CMDs with radii of 200 and 950 pixels for the cluster core and core plus corona regions, respectively (upper panels), and $r > 1000$ pixels for the star field region (lower right panel). The radius of the smallest circular extraction was fixed to guarantee the presence of a predominant number of cluster stars over field stars in the extracted CMD. The $r <$ 950 pixel CMDs were used to obtain a better definition of the fiducial cluster sequence from a larger number of cluster stars. Although

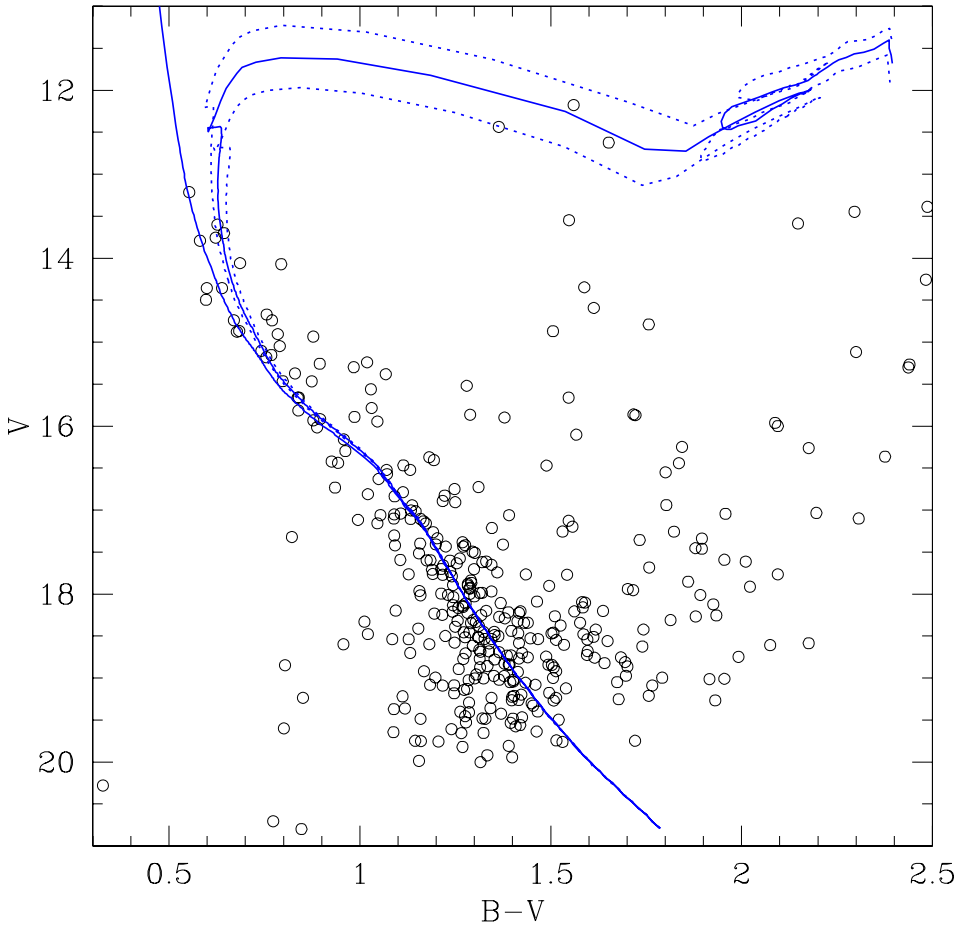

Figure 8. Field cleaned $(V, B-V)$ colour–magnitude diagram for stars in NGC 5288. The zero-age main sequence and the isochrones of $\log t = 8.00$, 8.10 and 8.20 from Lejeune & Schaerer (2001), computed taking into account overshooting and $Z = 0.04$, are overplotted.

cluster stars could be distributed through the entire observed field, there was little chance of finding them prevailing along the field edges over field stars.

The different sequences of the cluster core ($r < 200$ pixels) and field CMDs are not noticeable at all. In order to make the offsets from them more evident, we first overplotted the fitted zero-age main sequence (ZAMS) of Lejeune & Schaerer (2001) – more details are described in Section 5 – on the upper left CMDs. Then, we drew by eye the field star sequences using the lower right extracted CMDs and, finally, we added the adjusted ZAMS to these extracted field CMDs. As can be seen, the differences between the two sequences are $\Delta(B-V) \sim 0.1$–0.2 mag and $\Delta(V-I) \sim 0.2$–0.3 mag.

By using the lower right panel as the surrounding cluster field CMD, we applied a cleaning process to the $r < 950$ pixel CMDs in order to recover as many observed cluster stars as possible. First, we divided the field CMD into boxes of 0.25 mag in V and 0.10 mag in $B-V$ and $V-I$. We then counted the number of stars in each box and subtracted from the circular extraction CMDs a number of stars ($N_{i,j}$) given by the expression

$$N_{i,j} = (A_i/A_{\rm f})N_{{\rm f},j},$$

where $N_{{\rm f},j}$ is the number of field stars counted in the jth box, and $A_{\rm f}$ and A_i represent the areas covered by the surrounding field and circular extraction, respectively. The method assumes a uniform distribution over the entire field of stars of any spectral type. In Figs 6 and 7, the upper right and lower left panels illustrate the performance of this method, and show the $r < 950$ pixel CMDs before and after the cleaning process. As can be seen, although a high percentage of the field stellar population was removed, particularly for $V > 16$ mag, the residuals are still important for brighter stars. Therefore, with the aim of estimating the cluster fundamental parameters, we chose the $r < 200$ pixel CMDs, since we could thus achieve a reasonable balance between maximizing the cluster stars necessary to define the fiducial cluster sequence and minimizing field star contamination. Note that most bright stars defining the cluster turnoff are not spread all over the cluster area, core plus corona, but are concentrated in the core region.

5 CLUSTER FUNDAMENTAL PARAMETER ESTIMATES

The widely used procedure of fitting theoretical isochrones to the observed CMDs was employed to estimate the $E(B-V)$ and $E(V-I)$ colour excesses, the $V - M_V$ apparent distance modulus, and the age and the metallicity of NGC 5288. We fitted theoretical isochrones computed by Lejeune & Schaerer (2001) to the observed $(V, B-V)$ and $(V, V-I)$ CMDs. The isochrones, which cover an age range of 10^3 yr to 16–20 Gyr in steps of $\Delta \log t = 0.05$ dex, were calculated for the entire set of non-rotating Geneva stellar evolution models, covering masses from 0.4–0.8 to 120–150 $M_\odot$ and metallicities from $Z = 0.0004$ to 0.1. When selecting subsets of isochrones for different Z values to assess the metallicity effect in the cluster

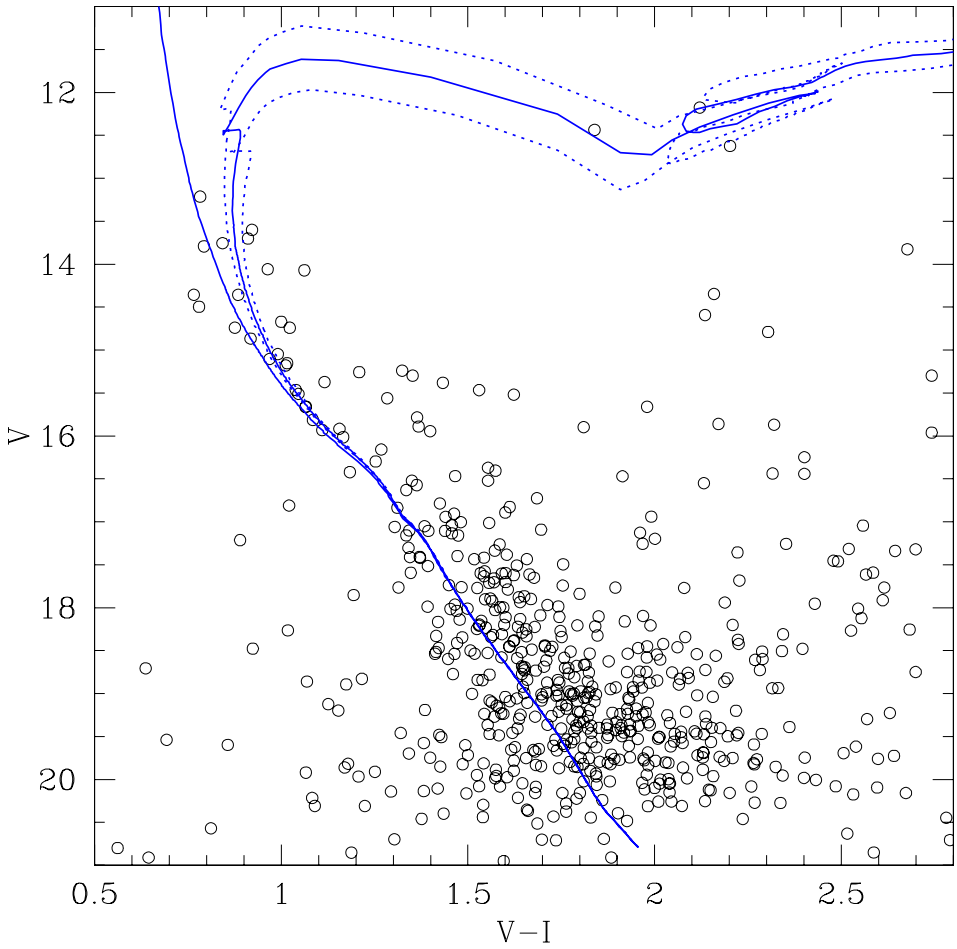

Figure 9. Field cleaned $(V, V-I)$ colour–magnitude diagram for stars in NGC 5288. The zero-age main sequence and the isochrones of $\log t = 8.00$, 8.10 and 8.20 from Lejeune & Schaerer (2001), computed taking into account overshooting and $Z = 0.04$, are overplotted.

fundamental parameters, we preferred those including the overshooting effect. Since there is no previous estimate of the cluster metal content available, we followed the general rule of starting by adopting no prearranged metallicity, but chemical compositions of $Z = 0.008$, 0.020 and 0.040 for the isochrone sets.

First, we independently fitted the ZAMS to the $(V, B-V)$ and $(V, V-I)$ CMDs for each selected metallicity and derived the cluster colour excesses $E(B-V)$ and $E(V-I)$ and the apparent distance modulus $V - M_V$. The relatively observed long cluster MS allowed these parameters to be satisfactorily determined. However, although the ZAMSs for the three distinct metallicities fit the lower MS very well, that for $Z = 0.040$ is the one which, as expected, best continues the non-evolved star sequence. Both metal-poorer ZAMSs turn out to be bluer at intermediate and upper magnitudes, even though the differences in colour excesses and apparent distance moduli are within 1σ of the derived parameter errors. Still, we decided to use the isochrones corresponding to $Z = 0.040$ for the subsequent analysis. Note that $Z = 0.040$ implies [Fe/H] $= +0.3$, if equation (11) of Bertelli et al. (1994) is used.

Next, we selected isochrones of $\log t$ larger than 8.0 and used the derived pair of $(V - M_V, E(B-V))$ and $(V - M_V, E(V-I))$ values to estimate the cluster age. The isochrone of $\log t = 8.10$ ($t = 130$ Myr) turned out to be the one which most accurately reproduces the cluster features in the $(V, B-V)$ and $(V, V-I)$ CMDs. To match this isochrone, we used $E(B-V)$ and $E(V-I)$ colour excesses and a $V - M_V$ apparent distance modulus of 0.75, 0.95 and 14.00, respectively, which were derived from the fit of the ZAMS. The uncertainties of these parameters were estimated from the individual values obtained from the cluster feature dispersion. Thus, we estimated $\sigma(E(B-V)) = \sigma(E(V-I)) = 0.05$ mag, $\sigma(V - M_V) = 0.25$ mag and $\sigma(t) = ^{+40}_{-30}$ Myr. In Figs 8 and 9 we overplotted the ZAMS and the isochrone of $\log t = 8.10$ (solid lines) for $Z = 0.040$ on to the cluster CMDs, and two additional isochrones of $\log t = 8.00$ and 8.20 for comparison purposes (dotted lines).

The possibility of estimating $E(B-V)$ and $E(V-I)$ independently allowed for their ratio to be computed, resulting in $E(V-I)/E(B-V) = 1.27 \pm 0.09$. When comparing this value with the value 1.25 from the normal interstellar extinction law (Dean, Warren & Cousins 1978), we found excellent agreement. Therefore, we used the derived reddenings and apparent distance modulus and the most frequently used values for the $A_V/E(B-V)$ ratio (Straizys 1992) to obtain $V_o - M_V = 11.6 \pm 0.3$, which implies a distance from the Sun of 2.1 ± 0.3 kpc and 91 pc below the Galactic plane. The distance error was computed with the expression:

$$\sigma(d) = 0.46[\sigma(V - M_V) + 3.2\sigma(E(B-V))] \times d,$$

where $\sigma(V - M_V)$ and $\sigma(E(B-V))$ represent the estimated errors in $V - M_V$ and $E(B-V)$, respectively. By using the cluster Galactic coordinates (l, b) and the calculated distance, we derived (7.18, −1.63, −0.09) kpc and ∼7.4 kpc for its (X, Y, Z) coordinates and

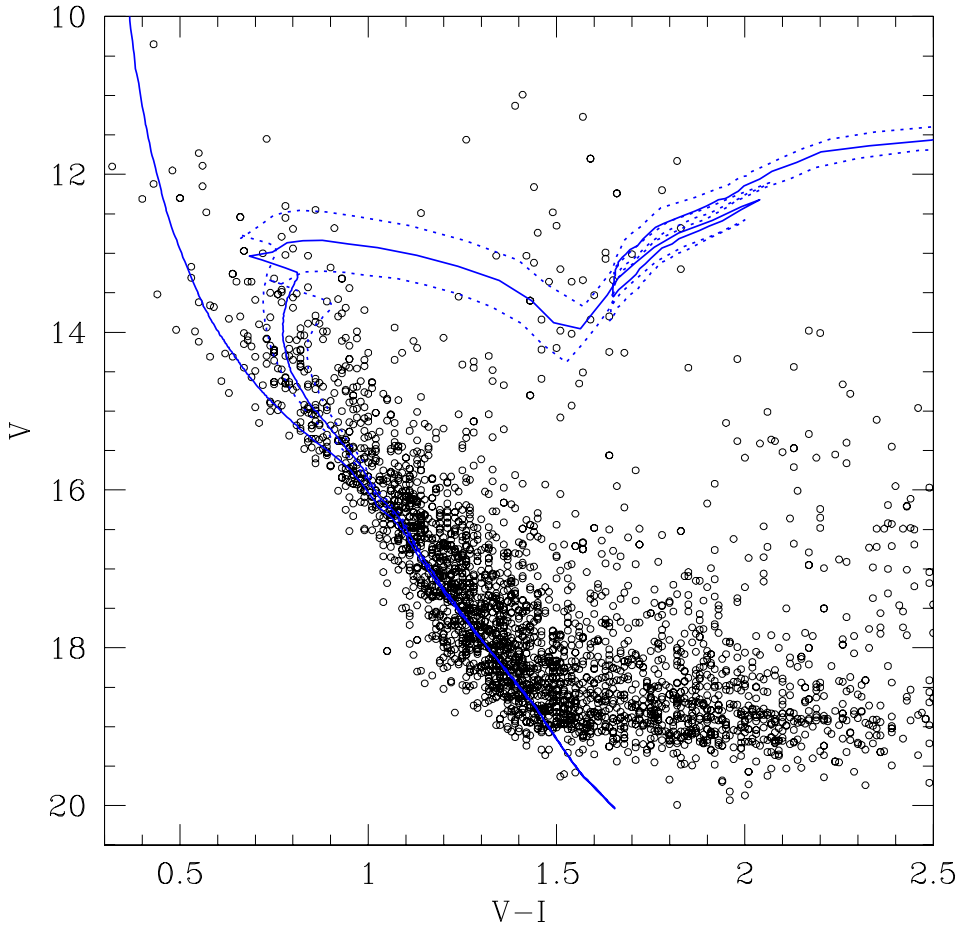

Figure 10. The $(V, V-I)$ colour–magnitude diagram for stars in NGC 5381 observed by Pietrzyński et al. (1997). The zero-age main sequence and the isochrones of $\log t = 8.55$, 8.65 and 8.75 from Lejeune & Schaerer (2001), computed taking into account overshooting and $Z = 0.04$, are overplotted.

Galactocentric distance, respectively, assuming the Sun's distance from the centre of the Galaxy to be 8.5 kpc.

6 NGC 5288: A NOT UNUSUAL OPEN CLUSTER

With the aim of locating NGC 5288 in the general framework of the structure and evolution of the Galactic disc, we first searched for clusters located at $(l, b)_{\rm cluster} = (l, b)_{\rm NGC5288} \pm 5^\circ$ in order to investigate the absorption extinction law along the line of sight of NGC 5288. We consider the WEBDA Open Cluster Database[1] to be an excellent tool to analyse cluster samples, since it is updated periodically. Thus, we searched WEBDA for open clusters with well-determined $E(B-V)$ colour excesses and distances from the Sun. When any of such quantities was not provided by WEBDA, we appealed to the most recent literature available. We found a sample of 28 open clusters within the desired (l, b) range which have well-determined fundamental parameters.

NGC 5381 is also an open cluster located within the required solid angle from the Sun towards NGC 5288 and not included in the sample of 28 clusters. Pietrzyński et al. (1997) mentioned that the cluster was identified by Lyngå (1972) and, to their knowledge, it was never studied photometrically. Thus, they conducted CCD *VI* observations with the aim of searching variable stars in the field of the cluster. Their fig. 2 presents the resulting $(V, V-I)$ CMD, which seems adequate to employ in estimating the cluster colour excess $E(V-I)$ and distance. However, the authors did not go into that process (see e.g. Dias et al. 2002; Chen et al. 2003). Thus, we used their observed cluster CMD to obtain those parameters following the same method described in Section 4. We obtained $E(V-I) = 0.65 \pm 0.05$ and $V - M_V = 13.25 \pm 0.25$, which turned into $E(B-V) = 0.52 \pm 0.05$ and $d = 2.1 \pm 0.4$ kpc, if we assume $E(V-I)/E(B-V) = 1.25$ (Dean et al. 1978) and $A_V/E(B-V) = 3.2$ (Straizys 1992). NGC 5381 turned out to be 450 ± 100 Myr old and relatively metal-rich ($Z = 0.04$). Fig. 10 shows the cluster CMD with the ZAMS and the isochrone of $\log t = 8.65$ superimposed (solid lines), and two additional isochrones of $\log t = 8.55$ and 8.75 (dotted lines) for comparison purposes. By adding this cluster to the above-mentioned list, we achieved a total of 29 open clusters with well-determined parameters located along the line of sight of NGC 5288.

The top left panel of Fig. 11 shows the distribution of the selected clusters and NGC 5288 in the Galactic (X, Y) plane, represented by open circles and by an open star, respectively. With the aim of achieving a better spatial resolution in the figure, we indicate with an arrow the farthest open cluster, BH 144, located at 12 kpc from the Sun (Carraro & Munari 2004). Note that the distance between the outermost and innermost clusters is nearly 12 kpc and that NGC 5288 is located behind the Carina spiral arm. The top right

[1] See http://obswww.unige.ch/webda/navigation.html

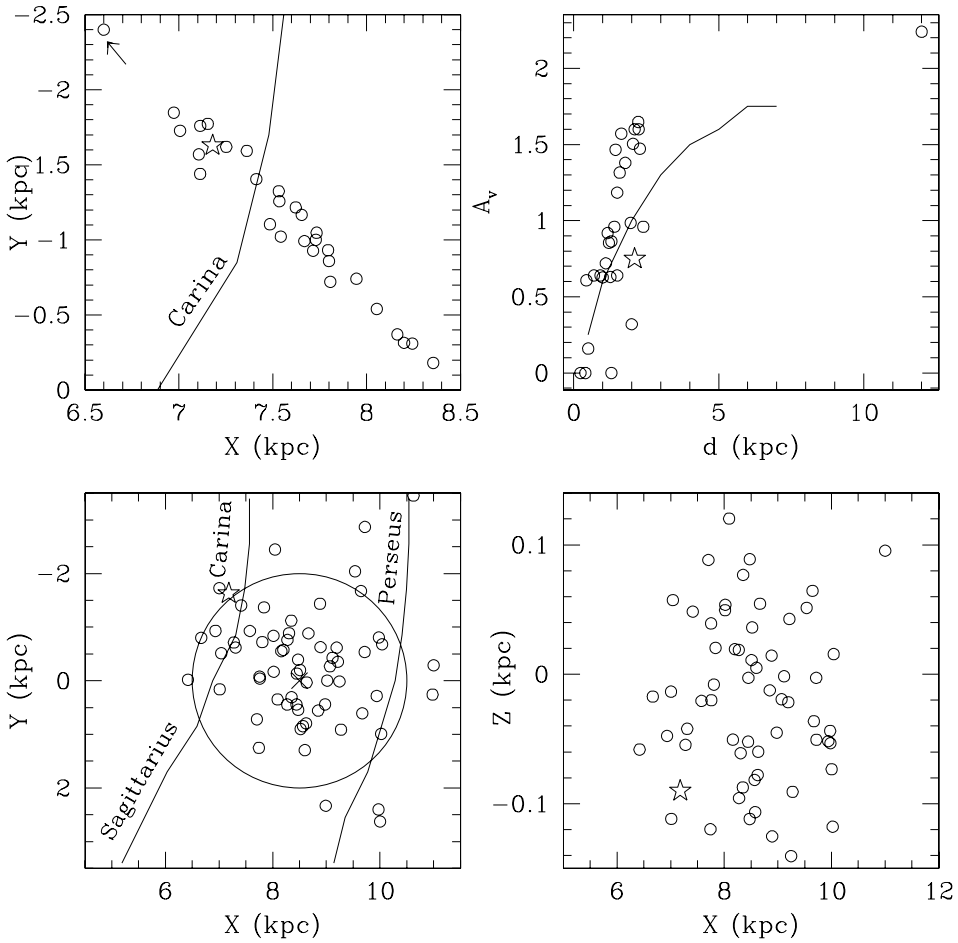

Figure 11. Top: Relationship between the Galactic coordinates X and Y (left), and the distance from the Sun and the visual interstellar absorption of open clusters located in the direction towards NGC 5288, with well-known fundamental parameters (right). Selected clusters and NGC 5288 are represented by open circles and by an open star, respectively. Bottom: Relationship between the Galactic coordinates X, Y and Z of open clusters with ages in the range $\log t =$ 8.0–8.2. Symbols are the same as in the top panels. A circle of 2 kpc radius centred at the Sun's position is drawn in the bottom left panel.

panel shows the relationship between the visual interstellar absorption A_V and the distance d from the Sun. For the sake of comparison, we also included the relationship for Baade's window [$(l, b) = (1^\circ, -3.9^\circ)$] obtained by Ng et al. (1996), which is represented by the solid line. Although results from clusters placed beyond 3 kpc from the Sun are needed for a sounder conclusion, the interstellar absorption in the direction of NGC 5288 appears not to be much more pronounced than the one along the direction of Baade's window. Bearing in mind this result and the fact that NGC 5288 is a relatively bright object, we think that the only estimate of the fundamental properties of the cluster results in a contribution to our knowledge of the Galactic open cluster system.

We also searched for clusters with ages similar to that of NGC 5288, i.e. $8.0 < \log t < 8.2$, in order to get an instantaneous picture of the Galactic disc in that epoch. Moreover, since the clusters are relatively young ($\sim$130 Myr), they could not have moved far away from their birthplaces. We found a total of 66 clusters, whose distribution in the Galactic (X, Y) plane is displayed at the bottom left panel of Fig. 11. The positions of the NGC 5288-like age clusters and NGC 5288 itself are represented by open circles and an open star, respectively. We also indicate the position of the Sun with a cross and draw a circle of 2 kpc radius from the Sun. Note that NGC 5288 is one of the two most distant inner disc clusters (we use the solar circle to distinguish between inner and outer disc clusters), the other one being Lyngå 1. The bottom right panel shows the clusters projected on to the Galactic (Z, X) plane. By looking at both bottom panels, we conclude that clusters of that age range did not form preferentially along the Galactic spiral arms, but in the thin Galactic disc ($Z \sim \pm$ 100 pc).

7 SUMMARY AND CONCLUSIONS

In this paper we present new CCD V magnitudes and $B - V$ and $V - I$ colours obtained in a 13.6 × 13.6 arcmin^2 field centred on the previously unstudied, relatively bright Galactic open cluster NGC 5288. This object is found to be a rich and strongly absorbed open cluster located beyond the Carina spiral feature. The analysis of the present photometric data leads to the following main conclusions:

(i) NGC 5288 appears to have a relatively small but conspicuous nucleus and a low-density extended corona. Star counts carried out in 25-pixel a side boxes distributed throughout the whole observed field allowed us to estimate the angular core and corona radii as $\sim$1.3 arcmin (0.8 pc) and 6.3 arcmin (3.8 pc), respectively. The confirmed existence of the coronal region is particularly important, since nearly 75 per cent of the cluster members lie in this region.

(ii) Estimates of the cluster fundamental parameters were performed from comparison of the observed $(V, B-V)$ and $(V, V-I)$ CMDs with theoretical isochrones of the Geneva group. For $Z = 0.040$ (equivalent to [Fe/H] $= +0.3$), the best-fitting isochrone yields $E(B-V) = 0.75 \pm 0.05$, $E(V-I) = 0.95 \pm 0.05$, $V - M_V = 14.00 \pm 0.25$ and an age of 130^{+40}_{-30} Myr. These results place NGC 5288 at a distance of 2.1 ± 0.3 kpc from the Sun and $\sim$7.4 kpc from the Galactic Centre. The vertical distance below the Galactic plane is 0.9 kpc, which indicates that NGC 5288 belongs to the thin disc. The cluster metallicity seems to be compatible with the widely recognized existence of a radial abundance gradient in the Galactic disc, the inner regions being metal richer than the outer ones.

(iii) Using the observed $(V, V-I)$ CMD of the open cluster NGC 5381 published by Pietrzyński et al. (1997), we derived, for the first time, the following basic parameters for this object nearly aligned along the line of sight of NGC 5288: $E(V-I) = 0.65 \pm 0.05$, $E(B-V) = 0.52 \pm 0.05$ and $V - M_V = 13.25 \pm 0.25$ ($d = 2.1 \pm 0.4$ kpc) for $\log t = 8.65$ ($t = 450 \pm 100$ Myr) and $Z = 0.040$.

(iv) The law of interstellar extinction in the direction of NGC 5288 is found to be normal. In particular, the visual interstellar absorption in this direction does not seem to be much more pronounced than the one along the direction of Baade's window.

(v) A comparison with 66 open clusters of nearly the same age as NGC 5288 reveals that the latter is one of the two most distant inner disc clusters of this age. Evidence is also presented in the sense that these NGC 5288-like age clusters did not form preferentially along the Galactic spiral arms but rather in the thin Galactic disc ($Z \sim \pm$ 100 pc).

ACKNOWLEDGMENTS

This work is based on observations made at the Cerro Tololo Inter-American Observatory (CTIO), which is operated by AURA, Inc., under cooperative agreement with the National Science Foundation. We appreciate the valuable comments and suggestions of the referee, Dr Jean-Claude Mermilliod. The present work was partially supported by the Argentinian institutions CONICET, Agencia Nacional de Promoción Científica y Tecnológica (ANPCyT), and Agencia Córdoba Ciencia.

REFERENCES

Alter G., Ruprecht J., Vanisek J., 1970, Catalogue of Star Clusters and Associations. Akademiai Kiado, Budapest
Archinal B. A., Hynes S. J., 2003, Star Clusters. Willman-Bell, Richmond, VA
Barkhatova M. M., 1950, Sov. Astron., 27, 184
Bertelli G., Bressan A., Chiosi C., Fagoto F., Nasi F., 1994, A&A, 106, 275
Carraro G., Munari U., 2004, MNRAS, 347, 625
Chen L., Hou J. L., Wang J. J., 2003, AJ, 125, 1397
Chupina N. V., Vereshchagin S. V., 1998, A&A, 334, 552
Collinder P., 1931, Medd. Lunds. Astron. Obs., 2
Dean F. J., Warren P. R., Cousins A. W. J., 1978, MNRAS, 183, 569
Dias W. S., Alessi B. S., Moitinho A., Lépine J. R. D., 2002, A&A, 389, 871
Friel E. D., 1995, ARA&A, 33, 381
Friel E. D., Janes K. A., 1993, A&A, 267, 75
Hogg A. R., 1965, Mem. Mount Stromlo Obs., 17
Janes K. A., Adler D., 1982, ApJS, 49, 425
Lejeune T., Schaerer D., 2001, A&A, 366, 538
Lyngå G., 1972, A&AS, 6, 327
Lyngå G., 1987, Catalogue of Open Cluster Data. Centre de Données Stellaires, Strasbourg
Mermilliod J.-C., 2005, WEBDA Open Cluster Database, http:/obswww.unige.ch/webda/
Ng Y. K., Bertelli G., Chiosi C., Bressan A., 1996, A&A, 310, 771
Nilakshi Sagar R., Pandey A. K., Mohan V., 2002, A&A, 383, 153
Piatti A. E., Clariá J. J., Ahumada A. V., 2003a, MNRAS, 344, 965
Piatti A. E., Clariá J. J., Ahumada A. V., 2003b, MNRAS, 346, 390
Piatti A. E., Clariá J. J., Ahumada A. V., 2004a, A&A, 418, 979
Piatti A. E., Clariá J. J., Ahumada A. V., 2004b, A&A, 421, 991
Piatti A. E., Clariá J. J., Ahumada A. V., 2004c, MNRAS, 349, 641
Piatti A. E., Clariá J. J., Ahumada A. V., 2005, PASP, 117, 22
Piatti A. E., Clariá J. J., Ahumada A. V., 2006, New Astron., 11, 262
Pietrzyński G., Kubiak M., Udalski A., Szymański M., 1997, Acta Astron., 47, 437
Ruprecht J., 1966, Bull. Astron. Inst. Czech., 17, 33
Straizys V., 1992, Multicolor Stellar Photometry. Pachart, Tucson, AZ
Trumpler R. J., 1930, Lick Obs. Bull., 14, 154
van den Bergh S., Hagen G. L., 1975, AJ, 80, 11

SUPPLEMENTARY MATERIAL

The following supplementary material is available for download as part of the full-text version of this article from http://www.blackwell-synergy.com:

Table 1. Sample CCD BVI data of stars in the field of NGC 5288.

This paper has been typeset from a TEX/LATEX file prepared by the author.